J Biomol NMR (2009) 44:113–118
DOI 10.1007/s10858-009-9317-z

NMR STRUCTURE NOTE

The NMR structure of the TC10- and Cdc42-interacting domain of CIP4

Yoshihiro Kobashigawa · Hiroyuki Kumeta · Daisuke Kanoh · Fuyuhiko Inagaki

Received: 27 January 2009 / Accepted: 6 April 2009 / Published online: 22 April 2009

Keywords CIP4 · Coiled-coil · GAPEX-5 · GLUT4 · Insulin

Biological context

Insulin stimulates glucose transport into striated (skeletal and cardiac) muscle and adipose tissue via the insulin-responsive glucose transporter GLUT4 (Chang et al. 2004). Since GLUT4 is continually recycled between general endocytotic compartments and specialized GLUT4 storage compartments (Bryant et al. 2002; Watson et al. 2004), the vast majority of GLUT4 resides within the cell in the basal state. Activation of insulin receptors by insulin binding triggers the relocation of GLUT4 vesicles to the cell surface (Jhun et al. 1992; Czech and Buxton 1993; Yang and Holman 1993). This increases the amount of GLUT4 on the plasma membrane and enhances glucose uptake into adipocytes and muscle cells (Bryant et al. 2002; Watson et al. 2004). CIP4 (Cdc42-interacting protein 4) was identified as a regulatory protein of GLUT4 relocation (Lodhi et al. 2007).

CIP4 contains an N-terminal FCH domain (the nonkinase domain of the FER and Fes/Fps family of tyrosine kinases) (Itoh et al. 2005), two central coiled-coil motifs and a C-terminal SH3 domain. The FCH domain together with the first coiled-coil motif interact with microtubules (Tian et al. 2000), while the second coiled-coil motif (comprising 332 to 425 of CIP4) is required for association with Rho-family GTPase proteins, Cdc42 (Aspenstrom 1997) and TC10 (Chang et al. 2002). The C-terminal SH3 domain associates with Gapex-5, a guanine nucleotide exchange factor for Rab31 (Lodhi et al. 2007). The CIP4 is predominantly located in intracellular compartments in adipocytes under basal conditions, but is relocated to the plasma membrane to bind GTP-loaded TC10 upon insulin stimulation (Chang et al. 2002). With the relocation of CIP4, Gapex-5 is also recruited to the plasma membrane. The Rab31 is found in the intracellular GLUT4-containing compartment, and is involved in the trafficking between endocytotic compartments and GLUT4 storage compartments (Lodhi et al. 2007). Translocation of the CIP4-Gapex-5 complex upon insulin stimulation abolishes the interaction of Gapex-5 with Rab31 and leads to a decrease in the amount of activated Rab31; therefore, it is thought to be one of the mechanisms by which the exocytosis of GLUT4-containing vesicles to the plasma membrane is increased (Lodhi et al. 2007).

Translocation of CIP4 is mediated by association with GTP-loaded TC10 localized at the plasma membrane. Insulin-stimulated activation of TC10 is indispensable for CIP4 translocation (Chang et al. 2002). Since the TC10 and Cdc42 binding region of CIP4 does not contain a known interaction motif that includes the CRIB (Cdc42 and Rac Interactive Binding) region (Chang et al. 2002), a plausible interaction mechanism remains elusive. Here, we report the solution structure of $CIP4_{332–425}$ and study the mode of interaction of $CIP4_{332–425}$ with both TC10 and Cdc42.

Electronic supplementary material The online version of this article (doi:10.1007/s10858-009-9317-z) contains supplementary material, which is available to authorized users.

Y. Kobashigawa · H. Kumeta · D. Kanoh · F. Inagaki (✉)
Laboratory of Structural Biology, Graduate School of Pharmaceutical Sciences, Hokkaido University, Sapporo, Hokkaido 060-0812, Japan
e-mail: finagaki@pharm.hokudai.ac.jp

Methods and results

The $CIP4_{332–425}$ was cloned into pGB1HPS (Kobashigawa et al. 2009) plasmid and expressed in *E. coli* at 25°C as GB1-fusion protein. The GB1, hexahistidine tags and a HRV3C protease cleavage site was fused to the N-terminus of $CIP4_{332–425}$. The protein was isotopically ^{13}C- and ^{15}N-labeled by growing an *E. coli* strain Rossetta2 (DE3) in M9 minimal medium containing $^{15}NH_4Cl$ (1 g/l) and ^{13}C-glucose (4 g/l) as sole nitrogen and carbon sources, respectively. Cells were grown at 37°C in M9 medium. Protein expression was induced by the addition of isopropyl-1-thio-β-galctopyranoside to a final concentration of 1 mM at 25°C. The cells were then cultured at 25°C and lysed. The GB1- and hexahistidine-tag fused $CIP4_{332–425}$ was purified using a Ni-NTA resin (Quiagen), and the GB1 and hexahistidine tags were cleaved from $CIP4_{332–425}$ with HRV3C protease. The $CIP4_{332–425}$ was then further purified using a Superdex75 gel filtration column (GE Healthcare Bio-Sciences). Finally, $CIP4_{332–425}$ was concentrated to 0.5 mM and applied to NMR experiments. All NMR measurements were carried out at 25°C and the sample was prepared in 20 mM MES buffer (pH 6.3) and 150 mM NaCl in the presence of 1 mM DTT. Using the same buffer as was used in the NMR experiments, we applied $CIP4_{332–425}$ to gel filtration chromatography and confirmed that $CIP4_{332–425}$ exists in monomer in solution (Supplementary Fig. 1). Retention time of $CIP4_{332–425}$ (11.5 kDa) was faster than GB1 (6.5 kDa), comparable with myoglobin (17.5 kDa) and slower than chymotripsinogen-A (25 kDa). As described below, $CIP4_{332–425}$ exhibits anisotropic structure with the long axis of 70 Å and the short axis of 27 Å, and is deviated from the globular shape and therefore, it is reasonable that $CIP4_{332–425}$ was eluted faster in gel filtration than expected from its molecular weight.

Two- and three-dimensional NMR experiments were performed on Varian UNITY Inova spectrometers operating at 800 and 600 MHz. Spectra were processed using the NMRPipe program (Delaglio et al. 1995) and data analysis was performed with the help of the Sparky program (Kneller and Goddard 1997). ^{1}H, ^{13}C and ^{15}N resonance assignments were carried out using the following suite of spectra; ^{1}H-^{15}N HSQC, ^{1}H-^{13}C HSQC, HN(CO)CA, HNCA, CBCA(CO)NH, HNCACB, HNCO, (HCA)CO(CA)NH, HBHA(CO)NH, HN(CA)HA, HC(C)H-TOCSY, (H)CCH-TOCSY, HbCbCgCdHd, HbCbCgCdCeHe, and HACAN. All the backbone amide proton and nitrogen resonances were assigned and nearly complete side-chain resonance assignments were accomplished. The ^{1}H, ^{13}C and ^{15}N chemical shifts were referenced to DSS according to IUPAC recommendations. Interproton distance restraints for structural calculations were obtained from ^{13}C-edited NOESY-HSQC and ^{15}N-edited NOESY-HSQC spectra using a mixing time of 100 ms. The structure was calculated using the CYANA 2.1 software package (Herrmann et al. 2002). A total of 2,325 distance restraints were used as input for the final calculation of the three-dimensional structure of $CIP4_{332–425}$ (Table 1). At each stage, 100 structures were calculated using 30,000 steps of simulated annealing, and a final ensemble of 20 structures was selected based on CYANA target function values. The atomic coordinates and resonance assignments have been deposited in the Protein Data Bank (PDB code: 2KE4) and BMRB (BMRB code: 16129), respectively.

The overlay of the final ensemble of 20 structures and the ribbon model of the lowest energy structure of $CIP4_{332–425}$ are shown in Fig. 1a, b, respectively. The N-terminal residues (332–338) exhibited flexible random structure characteristics. The core structure of $CIP4_{332–425}$ spanning 339–421 consists of two α-helices, which pack together into an anti-parallel coiled-coil structure. The packing between the two helices was mediated by a regular array of Leu, Ile and Val residues located at sites a and d of the chemical wheel (Fig. 1c).

To identify the TC10 and Cdc42 binding sites of $CIP4_{332–425}$, non-labeled GTPγS-loaded TC10 and Cdc42 were titrated to ^{15}N-labeled $CIP4_{332–425}$. The GB1-tagged $TC10_{1–185}$ and $Cdc42_{1–179}$ were prepared in a manner similar to $CIP4_{332–425}$ as described above. We used $TC10_{1–185}$ (Q67L) and $Cdc42_{1–179}$ (Q61L), constitutive active mutants that lack GTPase activity. GTPγS was loaded as described previously (Feltham et al. 1997). Upon addition of GTPγS-loaded $TC10_{1–185}$ (Q67L) and $Cdc42_{1–179}$ (Q61L), several amide peaks disappeared in an intermediate exchange process (Fig. 2a left and right panel). Almost identical peaks of $CIP4_{332–425}$ disappeared in both GTPγS-loaded $TC10_{1–185}$ (Q67L) and $Cdc42_{1–179}$ (Q61L) complexes, indicating that $CIP4_{332–425}$ binds to both activated G proteins using the same region. The peaks that disappeared at an equivalent

Table 1 Structural statistics of $CIP4_{332–425}$

NOE distance constraints	2,325
Short range (intraresidue and sequential)	1,403
Medium range ($2 \leq \|i–j\| \leq 4$)	627
Long range ($\|i–j\| > 4$)	295
Number of distance violations > 0.3 Å	0
Structural coordinates rmsd (Å)	
Backbone atoms	0.57
All heavy atoms	0.98
Ramachandran plot	
Most favored regions	86.0%
Additionally allowed regions	13.8%
Generously allowed regions	0.3%
Disallowed regions	0.0%

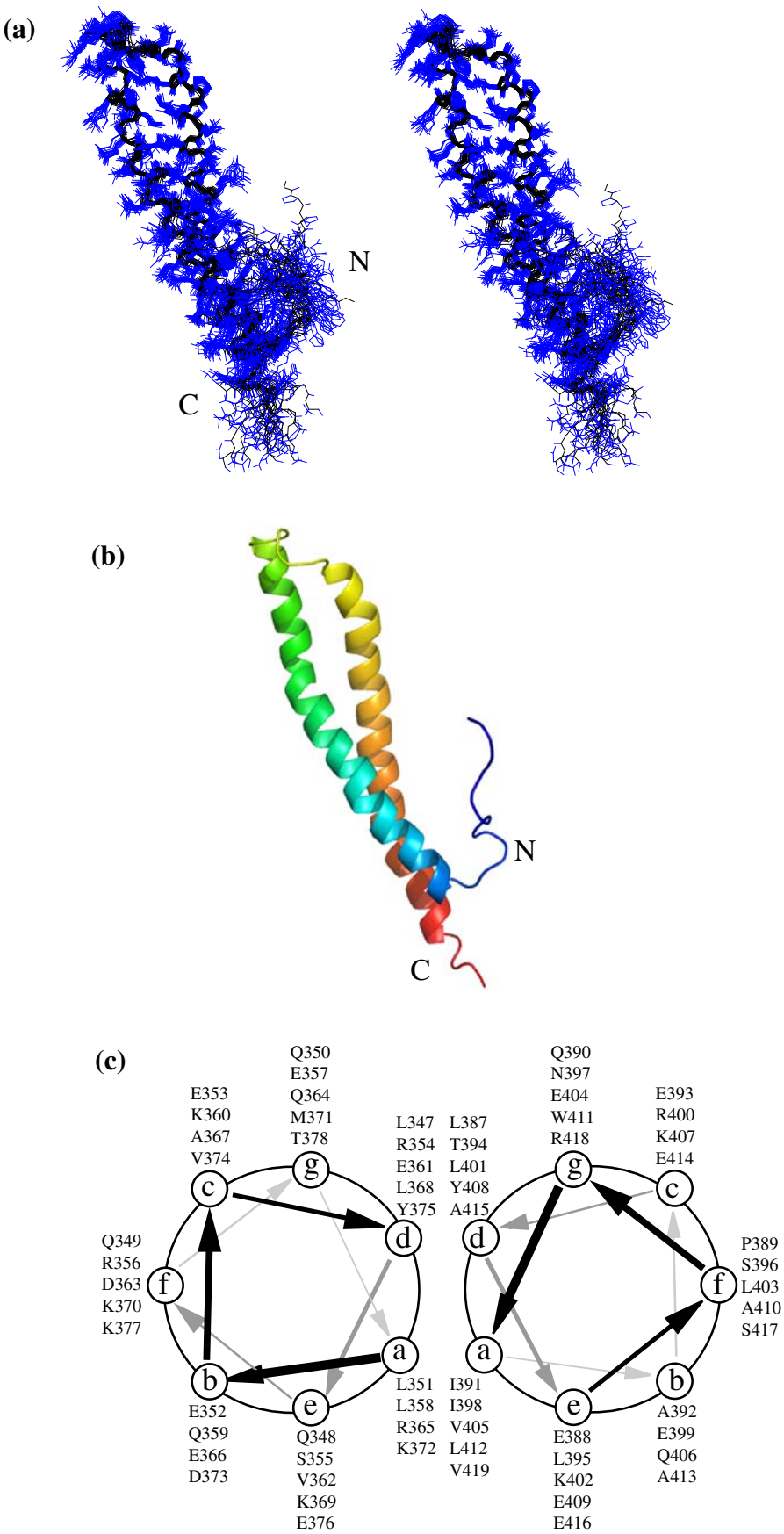

Fig. 1 Solution structure of $CIP4_{332–425}$. **a** Overlay of the ensemble of 20 final energy-minimized CYANA structures in stereo with heavy atoms from 339 to 421 being superimposed. The side chains are shown in *blue*. **b** Ribbon diagram of the lowest energy structure. **c** Wheel analysis of the coiled-coil of $CIP4_{332–425}$

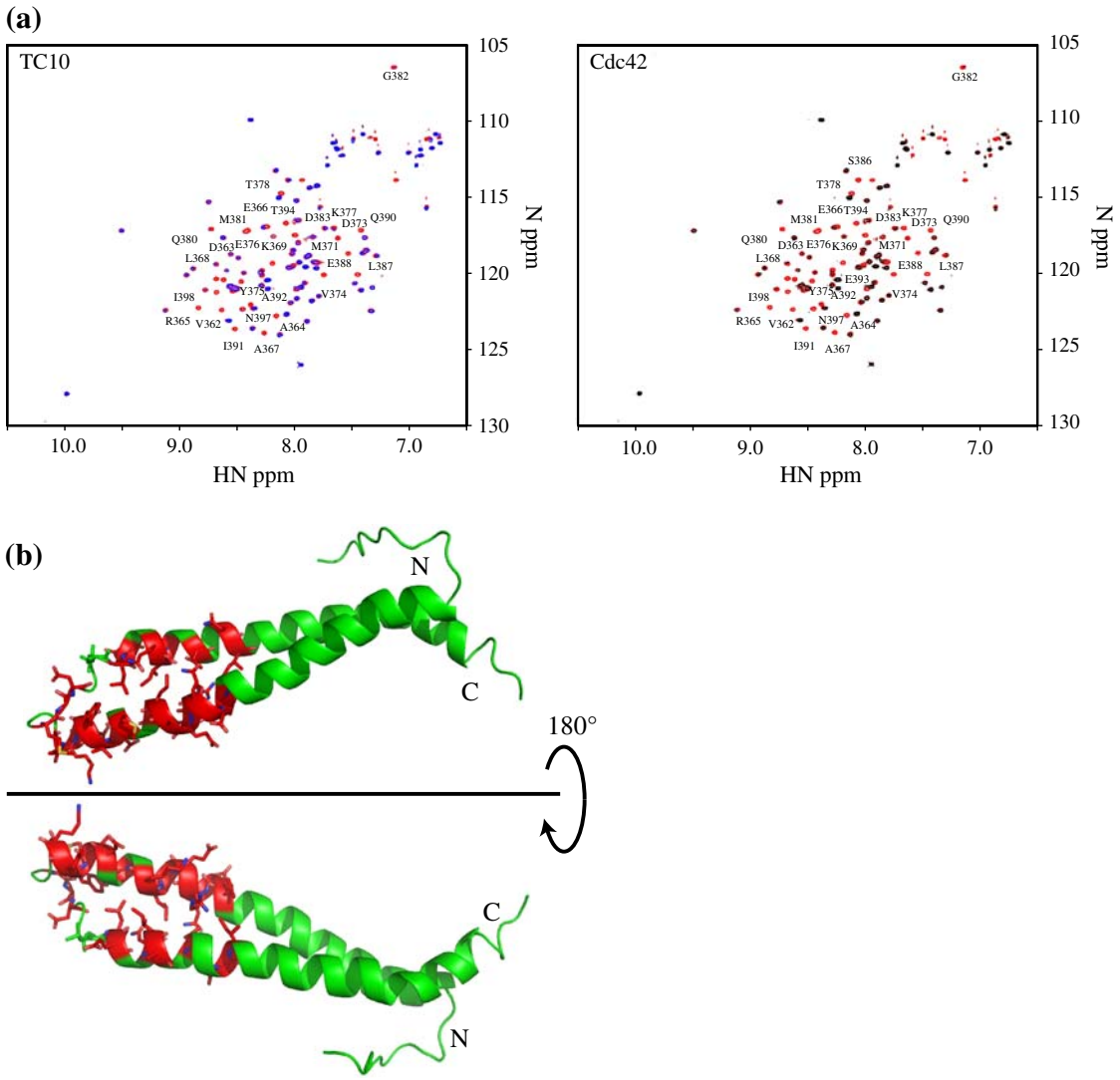

Fig. 2 **a** Overlay of the ^{1}H-^{15}N HSQC spectra of ^{15}N-labeled $CIP4_{332–425}$ in the absence (*red*) and presence of 1 molar equivalent of GTP-loaded $TC10_{1–185}$ (*blue* peaks in the *left panel*) and $Cdc42_{1–179}$ (*blue* peaks in the *right panel*). **b** Peaks that disappeared at 1 molar equivalent molar ratio of $TC10_{1–185}$ and $Cdc42_{1–179}$ to $CIP4_{332–425}$ were mapped on the structure of $CIP4_{332–425}$. The residues that disappeared are colored *red* and shown with a stick model

molar ratio of GTPase to $CIP_{332–425}$ were mapped on the $CIP4_{332–425}$ structure (Fig. 2b). They were located at the tip of the $CIP4_{332–425}$ that includes the C-terminal region of the first helix, the loop between the helices and the N-terminal region of the second helix. Most of the peaks disappeared due to precipitation of the sample at 1.5 equivalent molar ratio of GTPase to $CIP_{332–425}$, which prevents us from estimation of dissociation constant and observation of the NMR spectra at full saturation.

Discussion

We compared the structure of $CIP4_{332–425}$ with those deposited in the Protein Data Bank using the Dali search engine (Holm and Sander 1995). Both the protein kinase C-related kinase 1 (PRK1) HR1a domain bound to GTP-loaded RhoA (Maesaki et al. 1999; PDB code 1CXZ; Z score 7.8) and the HR1b domain associated with GTP-loaded Rac1 (Modha et al. 2008; PDB code 2RMK; Z score 7.1) showed a structure similar to $CIP4_{332–425}$. It should be noted that RhoA and Rac1 are classified into the Rho-family of small GTPase proteins like TC10 and Cdc42. HR1a and HR1b in complex form an anti-parallel coiled-coil structure with interfacial hydrophobic residues similar to that of $CIP4_{332–425}$ between the two helices. In the crystal structure of the RhoA-HR1a complex, HR1a binds to two different sites named contact I and contact II (Fig. 3a, b). On the other hand, the NMR structure of the Rac1-HR1b complex showed that HR1b binds to Rac1 at

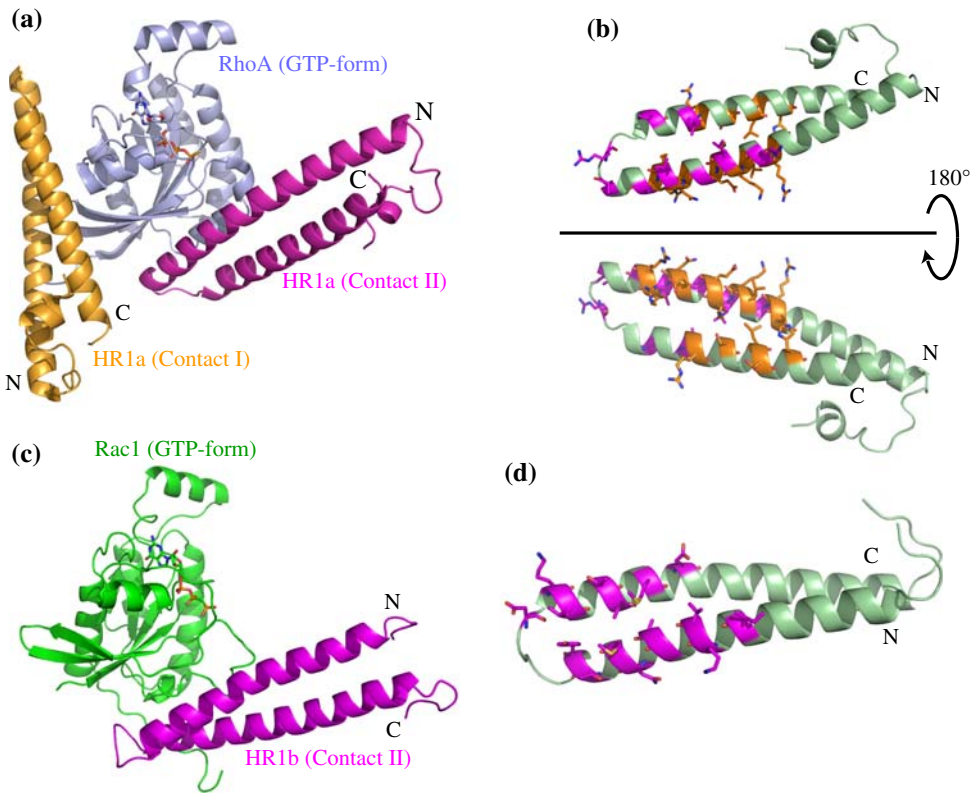

Fig. 3 Comparison of $CIP4_{332–425}$ with PRK HR1a and HR1b associated with Rho-family GTPases, RhoA and Rac1. **a** PRK HR1a complexed with RhoA (Maesaki et al. 1999; PDB code 1CXZ), and **b** the interaction sites of HR1a with RhoA. Interacting residues at contact I and contact II are colored *orange* and *magenta*, respectively, and their side chains are shown with a stick model. **c** PRK HR1b complexed with Rac1 (Modha et al. 2008; PDB code 2RMK; Z score 7.1), and **d** the interaction site of HR1b with Rac1. Interacting residues at contact II are colored *magenta* and their side chains are shown with a stick model

contact II (Fig. 3c, d). At contact I, HR1a binds to RhoA using the central region of the antiparallel coiled-coil structure, though using the opposite surface to that of contact II (Fig. 3b). At contact II, both HR1a and HR1b are bound to GTPases including the tip of the coiled-coil structure (Fig. 3b (upper), d). This is similar to the interaction of $CIP4_{332–425}$ with TC10 and Cdc42 identified from the present titration studies (Fig. 2a). Moreover, it should be noted that contact II extensively interacts with the switch I and switch II regions of RhoA and Rac1, while contact I does not (Supplementary Fig. 2 and 3). Since binding of Cdc42 and TC10 to $CIP4_{332–425}$ was reported to be GTP dependent (Aspenstrom 1997; Chang et al. 2002), contact II is more plausible as the binding site of $CIP4_{332–425}$. Considering the structure of $CIP4_{332–425}$ and the results of the titration experiment, it might be assumed that $CIP4_{332–425}$ binds both TC10 and Cdc42 at contact II. Further study, however, will be required including structure determination of the complex and the mutational analysis. Finally, this is the first report on the structure of the TC10 effector, which plays a crucial role in the translocation of GLUT4-containing vesicles to the plasma membrane to enhance glucose uptake in response to insulin stimulation.

Acknowledgments This work was supported (in part) by Targeted Proteins Research Program (TPRP) from Ministry of Education, Culture, Sports, Science and Technology (MEXT), Japan.

References

Aspenstrom P (1997) A Cdc42 target protein with homology to the non-kinase domain of FER has a potential role in regulating the actin cytoskeleton. Curr Biol 7:479–487

Bryant NJ, Govers R, James DE (2002) Regulated transport of the glucose transporter GLUT4. Nat Rev Mol Cell Biol 3:267–277

Chang L, Adams RD, Saltiel AR (2002) The TC10-interacting protein CIP4/2 is required for insulin-stimulated Glut4 translocation in 3T3L1 adipocytes. Proc Natl Acad Sci USA 99:12835–12840

Chang L, Chiang SH, Saltiel AR (2004) Insulin signaling and the regulation of glucose transport. Mol Med 10:65–71

Czech MP, Buxton JM (1993) Insulin action on the internalization of the GLUT4 glucose transporter in isolated rat adipocytes. J Biol Chem 268:9187–9190

Delaglio F, Grzesiek S, Vuister G, Zhu W, Pfeifer J, Bax A (1995) NMRPipe: a multidimensional spectral processing system based on UNIX pipes. J Biomol NMR 6:277–293

Feltham JI, Dotsch V, Raza S, Manor D, Cerione RA, Suteliffe MJ, Wagner G, Oswald RE (1997) Definition of the switch surface in the solution structure of Cdc42Hs. Biochemistry 36:8755–8766

Herrmann T, Guntert P, Wuthrich K (2002) Protein NMR structure determination with automated NOE assignment using the new software CANDID and the torsion angle dynamics algorithm DYANA. J Mol Biol 319:209–227

Holm L, Sander C (1995) Dali: a network tool for protein structure comparison. Trends Biochem Sci 20:478–480

Itoh T, Erdmann KS, Roux A, Habermann B, Werner H, De Camilli P (2005) Dynamin and the actin cytoskeleton cooperatively regulate plasma membrane invagination by BAR and F-BAR proteins. Dev Cell 9:791–804

Jhun BH, Rampal AL, Liu H, Lachaal M, Jung CY (1992) Effects of insulin on steady state kinetics of GLUT4 subcellular distribution

in rat adipocytes. Evidence of constitutive GLUT4 recycling. J Biol Chem 267:17710–17715

Kneller DG, Goddard TD (1997) SPARKY 3.105 edit. University of California, San Francisco

Kobashigawa Y, Kumeta H, Ogura K, Inagaki F (2009) Attachment of an NMR-invisible solubility enhancement tag using a sortase-mediated protein ligation method. J Biomol NMR 43:145–150. doi:10.1007/s10858-008-9296-5

Lodhi IJ, Chiang SH, Chang L, Vollenweider D, Watson RT, Inoue M, Pessin JE, Saltiel AR (2007) Gapex-5, a Rab31 guanine nucleotide exchange factor that regulates Glut4 trafficking in adipocytes. Cell Metab 5:59–72

Maesaki R, Ihara K, Shimizu T, Kuroda S, Kaibuchi K, Hakoshima T (1999) The structural basis of Rho effector recognition revealed by the crystal structure of human RhoA complexed with the effector domain of PKN/PRK1. Mol Cell 4:793–803

Modha R, Campbell LJ, Nietlispach D, Buhecha HR, Owen D, Mott HR (2008) The Rac1 polybasic region is required for interaction with its effector PRK1. J Biol Chem 283:1492–1500

Tian L, Nelson DL, Stewart DM (2000) Cdc42-interacting protein 4 mediates binding of the Wiskott-Aldrich syndrome protein to microtubules. J Biol Chem 275:7854–7861

Watson RT, Kanzaki M, Pessin JE (2004) Regulated membrane trafficking of the insulin-responsive glucose transporter 4 in adipocytes. Endocr Rev 25:177–204

Yang J, Holman GD (1993) Comparison of GLUT4 and GLUT1 subcellular trafficking in basal and insulin-stimulated 3T3–L1 cells. J Biol Chem 268:4600–4603